



Contents lists available at ScienceDirect

Bioorganic & Medicinal Chemistry Letters

journal homepage: www.elsevier.com/locate/bmcl

α -Aryl pyrrolidine sulfonamides as TRPA1 antagonists



Vishal A. Verma^{*}, Daniel G. M. Shore, Huifen Chen, Jun Chen, Steven Do, David H. Hackos, Aleks Kolesnikov, Joseph P. Lyssikatos, Suzanne Tay, Lan Wang, Anthony A. Estrada^{*}

Genentech, Inc., 1 DNA Way, South San Francisco, CA 94080, United States

ARTICLE INFO

Article history:

Received 21 September 2015

Revised 20 November 2015

Accepted 24 November 2015

Available online 25 November 2015

Keywords:

TRPA1

Metabolic stability

Ion channel

ABSTRACT

A series of α -aryl pyrrolidine sulfonamide TRPA1 antagonists were advanced from an HTS hit to compounds that were stable in liver microsomes with retention of TRPA1 potency. Metabolite identification studies and physicochemical properties were utilized as a strategy for compound design. These compounds serve as starting points for further compound optimization.

© 2015 Elsevier Ltd. All rights reserved.

The non-selective cation channel transient receptor potential ankyrin 1 (TRPA1) has been proposed as a polymodal irritant sensor of noxious exogenous [e.g., cinnamaldehyde, allyl-isothiocyanate (AITC), acrolein] and endogenous [4-hydroxynonenal (4-HNE), methylglyoxal, oxidized lipids] chemicals.¹ It is expressed predominantly in primary afferent nociceptive neurons in the dorsal root ganglia (DRG), trigeminal ganglia (TG), and nodose ganglia (NG).² The cryo EM single particle structure of TRPA1 was recently solved (~ 4 Å), and revealed a homotetrameric configuration with at least 16 ankyrin repeats in the N-terminal domain.³ Bridging the ankyrin repeats and the transmembrane domains (S1–S6) is a linker domain that possesses lysine and cysteine residues which play a critical role in channel activation through reaction with electrophilic ligands.¹ Multiple genetic studies have been reported that suggest TRPA1-dependent roles in neuropathic pain,^{4,5} asthma,^{6–8} and non-histaminergic itch.^{9,10} As a result, many academic and industrial groups have reported progress in the development of TRPA1 antagonists for the potential treatment of a variety of clinical indications including compounds that have progressed into the clinic.^{11–16}

As part of our own program targeting TRPA1 antagonists, compound **1** was identified through a high-throughput screening effort. In vitro evaluation of this compound indicated a moderate potency of 0.11 μ M against the human TRPA1 channel with a high $\log D$ ¹⁷ (4.4) resulting in a low lipophilic ligand efficiency (LLE) of 2.6. This series exhibited selectivity for TRPA1, as no activity was measured against the TRPV1, TRPC6 and TRPM8 channels. Initial efforts were directed towards improving the in vitro metabolic

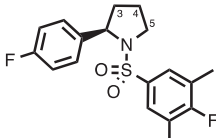
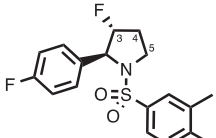
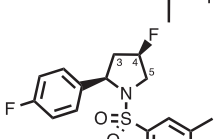
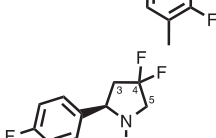
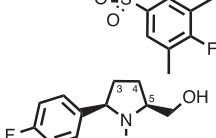
liability of this series, as the predicted hepatic clearance from both human and rat liver microsomes was high. Metabolite identification studies indicated that primary sites of metabolism were the methylenes of the pyrrolidine ring as well as the aryl sulfonamide. Sequential modifications were made in order to first probe the tolerance of these positions to change with respect to TRPA1 potency.

As such, a series of fluorinated pyrrolidine derivatives were synthesized in order to mitigate oxidative metabolism of the pyrrolidine methylenes as well as to decrease the $\log D$ of the compounds. Fluorination at the 3 position of the pyrrolidine ring led to an improvement in potency but no significant increase in metabolic stability (**2**, Table 1). While the measured $\log D$ of the 4-fluoro compound **3** indicated a decreased lipophilicity that translated into moderately improved stability, it was accompanied by a loss in potency. The 4-*gem*-difluoro target **4** was equipotent to 3-F compound **2** but led to a loss of the moderate stability gained in **3**. The 5 position of the pyrrolidine was probed in order to investigate a location for the installation of more polar groups to improve stability and solubility. Incorporation of a hydroxymethyl group at the 5 position (**5**) led to an increase in polarity as well as a small increase in potency but did not exhibit any improvement in stability. Nonetheless, these compounds indicated that mono-fluorination of the 3 position and di-fluorination of the 4 position on various scaffolds have the potential to lead to potency increases and so were envisioned to be combined with further modifications to impart an overall increase in metabolic stability while improving or maintaining potency.

The two fold increase in potency of the hydroxymethyl compound **5** prompted the synthesis of various derivatives at this position targeting compounds with improved physicochemical

^{*} Corresponding authors.

Table 1
TRPA1 antagonist logDs, potencies and liver microsome-predicted hepatic stability data for pyrrolidine modifications

Compd Structure	logD ^a	IC ₅₀ (μM)	HLM Cl ^b (mL/min/kg)	RLM Cl ^b (mL/min/kg)
	4.4	0.110	19	46
	3.9	0.020	18	36
	2.6	0.380	13	21
	4.2	0.023	19	45
	3.3	0.063	19	40

^a pH 7.4.

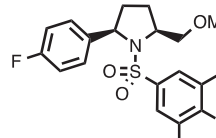
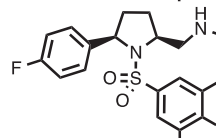
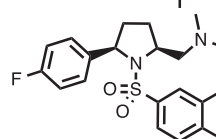
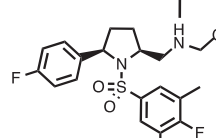
^b Human and rat predicted hepatic clearance using liver microsomes using the formula based on the well-stirred model: predicted hepatic Cl = (QH × f_{ub}LM × Cl_{int}) / (QH + f_{ub}LM × Cl_{int}) where QH is species liver blood flow, f_{ub}LM is fraction unbound in liver microsomes and in the absence of measured microsomal binding f_{ub}LM is assumed to equal 1.

properties. Capping the hydroxyl group as the methyl ether (**6**) led to a loss in potency (Table 2). Incorporation of basic amines as replacements for the hydroxyl group were not tolerated, as the *N*-methyl and *N,N*-dimethyl containing compounds **7** and **8** led to complete loss of activity. The less basic trifluoroethylamine **9** also was not tolerated. Additionally, the increased polarity of some of these compounds did not translate into improvements in metabolic stability.

Attention was next turned to the substituted phenylsulfonamide, as metabolite ID studies indicated this was a site of extensive metabolism. Targeting improved physicochemical characteristics, replacement of the phenyl group with a pyridyl functionality (**10** and **11**) led to loss of activity as well as no improvement in stability (Table 3). Conversion of the sulfonamide moiety to the amide **12** as well as the benzyl amine **13** also was not tolerated.

Derivatives of the substituents on the phenyl sulfonamide were next explored. Removal of the methyl groups as well as the fluorine by replacement with an unsubstituted phenyl group in **14** did lead to a more polar compound as expected (logD of 2.2 compared to 3.3) but also led to complete loss of activity (Table 4). Removal of only the 4-F substituent (**15**) led to a drop in potency while excision of a single methyl group (**16**) led to only a two-fold drop

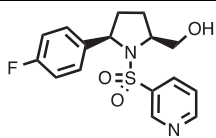
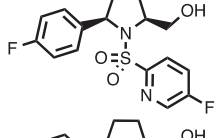
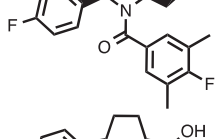
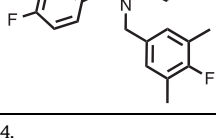
Table 2
TRPA1 antagonist logDs, potencies and liver microsome-predicted hepatic stability data for hydroxymethyl modifications

Compd Structure	logD ^a	IC ₅₀ (μM)	HLM Cl ^b (mL/min/kg)	RLM Cl ^b (mL/min/kg)
	3.9	0.270	19	45
	2.7	>20	12	53
	3.7	>18	18	42
	4.3	>20	18	37

^a pH 7.4.

^b Human and rat predicted hepatic clearance using liver microsomes using the formula based on the well-stirred model: predicted hepatic Cl = (QH × f_{ub}LM × Cl_{int}) / (QH + f_{ub}LM × Cl_{int}) where QH is species liver blood flow, f_{ub}LM is fraction unbound in liver microsomes and in the absence of measured microsomal binding f_{ub}LM is assumed to equal 1.

Table 3
TRPA1 antagonist logDs, potencies and liver microsome-predicted hepatic stability data for sulfonamide modifications

Compd Structure	logD ^a	IC ₅₀ (μM)	HLM Cl ^b (mL/min/kg)	RLM Cl ^b (mL/min/kg)
	1.1	>20	20	53
	2.0	>20	18	43
	3.1	>20	nm	nm
	4.0	6.7	nm	nm

^a pH 7.4.

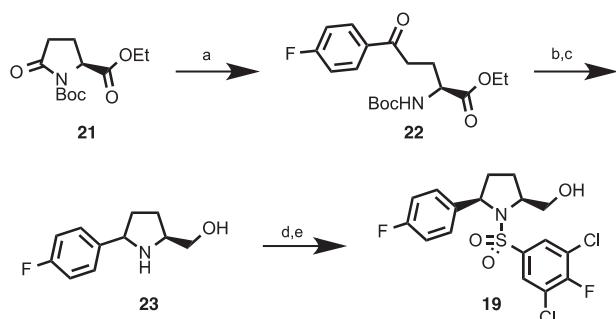
^b Human and rat predicted hepatic clearance using liver microsomes using the formula based on the well-stirred model: predicted hepatic Cl = (QH × f_{ub}LM × Cl_{int}) / (QH + f_{ub}LM × Cl_{int}) where QH is species liver blood flow, f_{ub}LM is fraction unbound in liver microsomes and in the absence of measured microsomal binding f_{ub}LM is assumed to equal 1.

Table 4
TRPA1 antagonist logDs, potencies and liver microsome-predicted hepatic stability data for aryl sulfonamide substituent modifications

Compd	Structure	logD ^a	IC ₅₀ (μM)	HLM Cl ^b (mL/min/kg)	RLM Cl ^b (mL/min/kg)
14		2.2	>19	20	53
15		3.2	0.290	19	28
16		2.8	0.190	18	37
17		3.2	6.6	nm	nm
18		3.6	0.130	19	40
19		3.8	0.110	7.3	13
20		4.6	0.350	6	12

^a pH 7.4.

^b Human and rat predicted hepatic clearance using liver microsomes using the formula based on the well-stirred model: predicted hepatic Cl = $(QH \times f_{ub}LM \times Cl_{int}) / (QH + f_{ub}LM \times Cl_{int})$ where QH is species liver blood flow, $f_{ub}LM$ is fraction unbound in liver microsomes and in the absence of measured microsomal binding $f_{ub}LM$ is assumed to equal 1.



Scheme 1. Synthesis of target compound **19**. Reagents and conditions: (a) 4-F-PhMgBr (1.2 equiv), 2-MeTHF, 0 °C, 30 min (91%); (b) TFA (4.0 equiv), CH₂Cl₂, 40 °C, 3 h; (c) NaBH₄ (6.0 equiv), MeOH (70% over two steps); (d) separation; (e) ArSO₂Cl (1.5 equiv), Et₃N (2.0 equiv), CH₂Cl₂, 16 h (39%).

in activity. However, removal of both methyl groups (in the C5 unsubstituted series) led to abrogation of potency (**17**). A key isosteric replacement of a methyl group with a chlorine in **18** indicated no loss in activity and thus compound **19** was next synthesized, replacing both methyl groups with chlorines. Compound **19** was equipotent to **1** but critically exhibited a significant improvement in metabolic stability in both human and rat liver microsomes. This result was also notable in that it appeared to obviate the need for fluoro substitution on the pyrrolidine ring for metabolic stability. This 3,5-dichloro-4-fluoro phenyl sulfonamide moiety was also placed on the initial pyrrolidine system lacking a C5 hydroxymethyl (**20**) but led to a three fold loss in activity. Importantly, however, compound **20** also displayed an increase in stability in the human and rat microsome assays relative to compound **1**, supporting the trend that the chlorine for methyl substitutions are able to ameliorate the metabolic liabilities with this series. It should be noted that it cannot be ruled out that potential differences in microsomal binding could account for this stability increase.

The synthesis of compound **19** began from the ethyl ester of *N*-Boc pyroglutamate (**21**, Scheme 1). Aryl Grignard addition gave ketone **22**, which was followed by Boc deprotection and subsequent cyclization. Reduction to amino alcohol **23** was accomplished with sodium borohydride. The diastereomers were separated and formation of the sulfonamide then resulted in the final compound **19**.

Additional evaluation of compound **19** indicated selectivity for the human TRPA1 channel over the rat channel as was typical for this series (Table 5). Moderate improvement of the logD from the initial hit had been achieved, resulting in a modest increase in the LLE. Hepatic clearance calculated from human and rat liver microsomes indicated relative stability in this in vitro assay. Potentially as a result of its moderate logD, compound **20** was membrane permeable, highly plasma protein bound and exhibited low kinetic aqueous solubility.

The progress described herein represents advancement of an HTS hit guided by physicochemical properties and utilizing both TRPA1 potency as well as in vitro evaluation of metabolic stability in liver microsomes to arrive at starting points for further compound optimization. Steep structure activity relationships in terms of both potency and metabolic stability have been established for many positions of these compounds. Areas for further refinement include increasing potency through increased LLE as well as increasing solubility by driving down logD.

Table 5
In vitro and physicochemical properties of compound **19**

Human TRPA1 IC ₅₀ (μM)	0.11
Rat TRPA1 IC ₅₀ (μM)	7.3
logD (pH 7.4)	3.9
LLE	3.1
HLM Cl ^a (mL/min/kg)	7.3
RLM Cl ^a (mL/min/kg)	13
MDCK (10 ⁻⁶ cm/s)	5.7
Human PPB (%)	99.4
Kinetic aqueous solubility (μM)	<1

^a Human and rat predicted hepatic clearance using liver microsomes using the formula based on the well-stirred model: predicted hepatic Cl = $(QH \times f_{ub}LM \times Cl_{int}) / (QH + f_{ub}LM \times Cl_{int})$ where QH is species liver blood flow, $f_{ub}LM$ is fraction unbound in liver microsomes and in the absence of measured microsomal binding $f_{ub}LM$ is assumed to equal 1.

Acknowledgement

We would like to thank Yanzhou Liu for help with NMR analysis.

References and notes

1. Chen, J.; Hackos, D. H. *Naunyn-Schmiedeberg's Arch. Pharmacol.* **2015**, *388*, 451.
2. Nagata, K.; Duggan, A.; Kumar, G.; García-Añoveros, J. *J. Neurosci.* **2005**, *25*, 4052.
3. Paulsen, C. E.; Armache, J.-P.; Gao, Y.; Cheng, Y.; Julius, D. *Nature* **2015**, *520*, 511.
4. Old, E. A.; Nadkarni, S.; Grist, J.; Gentry, C.; Bevan, S.; Kim, K.-W.; Mogg, A. J.; Perretti, M.; Malcangio, M. *J. Clin. Invest.* **2014**, *124*, 2023.
5. Trevisan, G.; Materazzi, S.; Fusi, C.; Altomare, A.; Aldini, G.; Lodovici, M.; Patacchini, R.; Geppetti, P.; Nassini, R. *Cancer Res.* **2013**, *73*, 3120.
6. Caceres, A. I.; Brackmann, M.; Elia, M. D.; Bessac, B. F.; del Camino, D.; D'Amours, M.; Witek, J. S.; Fanger, C. M.; Chong, J. A.; Hayward, N. J.; Homer, R. J.; Cohn, L.; Huang, X.; Moran, M. M.; Jordt, S.-E. *Proc. Natl. Acad. Sci. U.S.A.* **2009**, *106*, 9099.
7. Hox, V.; Vanoirbeek, J. A.; Alpizar, Y. A.; Voedisch, S.; Callebaut, I.; Bobic, S.; Sharify, A.; De Vooght, V.; Van Gerven, L.; Devos, F.; Liston, A.; Voets, T.; Vennekens, R.; Bullens, D. M. A.; De Vries, A.; Hoet, P.; Braun, A.; Ceuppens, J. L.; Talavera, K.; Nemery, B.; Hellings, P. W. *Am. J. Respir. Crit. Care Med.* **2013**, *187*, 486.
8. Nassini, R.; Materazzi, S.; Andre, E.; Sartiani, L.; Aldini, G.; Trevisani, M.; Carnini, C.; Massi, D.; Pedretti, P.; Carini, M.; Cerbai, E.; Preti, D.; Villetti, G.; Civelli, M.; Trevisan, G.; Azzari, C.; Stokesberry, S.; Sadofsky, L.; McGarvey, L.; Patacchini, R.; Geppetti, P. *FASEB J.* **2010**, *24*, 4904.
9. Wilson, S. R.; Gerhold, K. A.; Bifolck-Fisher, A.; Liu, Q.; Patel, K. N.; Dong, X.; Bautista, D. M. *Nat. Neurosci.* **2011**, *14*, 595.
10. Cevikbas, F.; Wang, X.; Akiyama, T.; Kempkes, C.; Savinko, T.; Antal, A.; Kukova, G.; Buhl, T.; Ikoma, A.; Buddenkotte, J.; Soumelis, V.; Feld, M.; Alenius, H.; Dillon, S. R.; Carstens, E.; Homey, B.; Basbaum, A.; Steinhoff, M. *J. Allergy Clin. Immunol.* **2014**, *133*, 448.
11. Preti, D.; Saponaro, G.; Szallasi, A. *Pharm. Pat. Anal.* **2015**, *4*, 75.
12. Copeland, K. W.; Boezio, A. A.; Cheung, E.; Lee, J.; Olivieri, P.; Schenkel, L. B.; Wan, Q.; Wang, W.; Wells, M. C.; Youngblood, B.; Gavva, N. R.; Lehto, S. G.; Geuns-Meyer, S. *Bioorg. Med. Chem. Lett.* **2014**, *24*, 3464.
13. Rooney, L.; Vidal, A.; D'Souza, A.-M.; Devereux, N.; Masick, B.; Boissel, V.; West, R.; Head, V.; Stringer, R.; Lao, J.; Petrus, M. J.; Patapoutian, A.; Nash, M.; Stoakley, N.; Panesar, M.; Verkuyl, J. M.; Schumacher, A. M.; Petrassi, H. M.; Tully, D. C. *J. Med. Chem.* **2014**, *57*, 5129.
14. Laliberté, S.; Vallée, F.; Fournier, P.-A.; Bedard, L.; Labrecque, J.; Albert, J. S. *Bioorg. Med. Chem. Lett.* **2014**, *24*, 3204.
15. Hu, Y.-J.; St-Onge, M.; Laliberté, S.; Vallée, F.; Jin, S.; Bedard, L.; Labrecque, J.; Albert, J. S. *Bioorg. Med. Chem. Lett.* **2014**, *24*, 3199.
16. Gijzen, H. J. M.; Berthelot, D.; De Cleyn, M. A. J.; Geuens, I.; Brône, B.; Mercken, M. *Bioorg. Med. Chem. Lett.* **2012**, *22*, 797.
17. Lin, B.; Pease, J. H. *Comb. Chem. High Throughput Screening* **2013**, *16*, 817.